ISSN 0023-1584, Kinetics and Catalysis, 2012, Vol. 53, No. 1, pp. 125–136. © Pleiades Publishing, Ltd., 2012.
Original Russian Text © A.A. Shutilov, G.A. Zenkovets, S.V. Tsybulya, V.Yu. Gavrilov, 2012, published in Kinetika i Kataliz, 2012, Vol. 53, No. 1, pp. 128–140.

Effect of Silica on the Stability of the Nanostructure and Texture of Fine-Particle Alumina

A. A. Shutilov[a, b], G. A. Zenkovets[a, b], S. V. Tsybulya[a, b], and V. Yu. Gavrilov[a]

[a] *Boreskov Institute of Catalysis, Siberian Branch, Russian Academy of Sciences, Novosibirsk, 630090 Russia*
[b] *Novosibirsk State University, Novosibirsk, 630090 Russia*
e-mail: zenk@catalysis.ru

Received March 11, 2011

Abstract—The effect of the modification of aluminum oxide with silicon oxide on the stability of fine-particle γ- and δ-Al_2O_3 phases upon heat treatment in the wide temperature range of 550–1500°C was studied. It was found that the γ- and δ-Al_2O_3 phases modified with silica are thermally stable up to higher temperatures than pure aluminum oxide. This is due to changes in the real structure of the modified samples, specifically, an increase in the concentration of extensive defects stabilized by hydroxyl groups bound to not only aluminum atoms but also silicon atoms. It is likely that Si–OH groups, which are thermally more stable than Al–OH groups, stabilize the microstructure of γ- and δ-Al_2O_3 to higher temperatures, as compared with aluminum oxide containing no additives. Simultaneously, an increase in the thermal stability of the modified samples is accompanied by the retention of a high specific surface area and a developed pore structure at higher treatment temperatures.

DOI: 10.1134/S0023158412010120

INTRODUCTION

Aluminum oxide is used as an adsorbent and support for metal and oxide catalysts employed both in the manufacture of valuable chemical substances and in environmental protection processes. For example, alumina is used in supported metal catalysts (Pt, Pd, and Ni/Al_2O_3) for hydrogenation, hydrogenolysis, and reforming processes [1] and also in Pt and Pd/Al_2O_3 catalysts for the neutralization of the harmful gas emissions of chemical enterprises and motor transport to remove nitrogen and carbon oxides [2–4]. Supports based on aluminum oxide are also used in supported Co(Ni)–Mo(W) sulfide catalysts for the hydrodesulfurization of diesel fuel [5].

Metastable forms with the structures of γ- and δ-Al_2O_3 are the most promising catalyst supports. These crystalline modifications possess a sufficiently high specific surface area and a developed pore structure, which make it possible to stabilize an active constituent on the surface in a fine-particle state to prevent its sintering at high temperatures. An increase in the temperature of heat treatment above 1000°C leads to the phase transformation of the γ- and δ-Al_2O_3 modifications into α-Al_2O_3. The phase transformation is accompanied by a sharp decrease in the specific surface area and porosity.

It was noted that the modification of aluminum oxide with silica leads to an increase in the thermal stability of its low-temperature modifications [6, 7]; however, the reasons for this phenomenon remain unclear until now. At the same time, aluminum oxide containing silicon oxide is frequently used as a support for different types of catalysts [8–11]. The cause of the increase in the thermal stability of γ- and δ-Al_2O_3 in the presence of silica can be elucidated by studying the structure formation of the modified aluminum oxide at different stages of its synthesis.

It was found [12–18] that the nature of the initial aluminum hydroxide compound (amorphous aluminum hydroxide, pseudoboehmite, boehmite, bayerite, and gibbsite) exerts a crucial effect on the formation of the metastable forms of aluminum oxide (γ-, η-, χ-, and θ-Al_2O_3) upon thermal treatment and on the temperature of their transition into α-Al_2O_3. Based on the X-ray diffraction and electron microscopic studies of the fine-particle metastable modifications of aluminum oxide [15–17], it was shown that the formation of alumina modifications (γ-, η-, χ-, and θ-Al_2O_3) is determined by the habitus (type of the developed face) of primary particles and by the method of their jointing with each other. Thus, for instance, the samples of γ-Al_2O_3 obtained from pseudoboehmite are the aggregates (>100 nm in size) of fine-particle (about 3 nm) oxide particles, disoriented relative to each other with the large angles of turn. The samples of γ-Al_2O_3 obtained from boehmite have the shape of extensive (approximately 100 nm in size) single-crystal plates with the most developed (110) face. Their main structural peculiarity is the presence of extensive defects as closed pseudohexagonal loops formed by vacancy

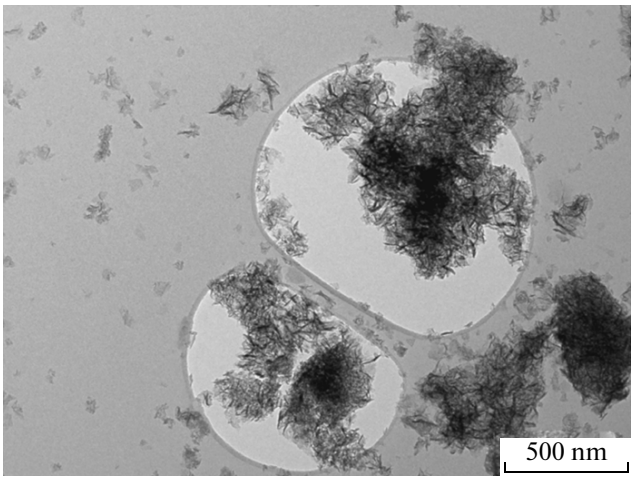

Fig. 1. Micrograph of the initial aluminum oxide.

walls, in which hydroxyl groups and water molecules are stabilized. During heat treatment, the gradual loss of residual hydroxyl groups occurs, causing a decrease in the concentration of related defects and then structure ordering with the formation of δ-Al_2O_3 followed by its transition to α-Al_2O_3.

Based on the above published data, we can hypothesize that the modification of aluminum oxide with silicon oxide will change the structure its metastable fine-particle forms, which, in turn, will have an effect on the thermal stability of the modified samples. Consequently, it is possible to assume that the development of the new types of fine-particle nanostructured materials on the basis of aluminum oxide, which are characterized by an increased thermal stability in comparison with the metastable modifications of aluminum oxide, should be preceded by a careful study of the formation of their real structure at the individual stages of the synthesis.

The aim of this work was to study the influence of the modification of aluminum oxide with silica on the structure, texture, and thermal stability of the fine-particle γ- and δ-Al_2O_3 modifications upon heat treatment.

EXPERIMENTAL

As the initial compound, $Al_2(SO_4)_3 \cdot 18H_2O$ of analytical grade was used. The samples of alumina were prepared by precipitation from an aqueous solution of aluminum sulfate with a 12.5% aqueous solution of ammonia at a constant value of pH 9 with the subsequent washing of the precipitate with distilled water until the absence of sulfate ions in the washwater. The resulting samples were dried in air to an air-dry state and then in a drying box at a temperature of 110°C for 12–14 h and calcined in a muffle furnace at 400–1200°C for 4 h.

The aluminum oxide samples dried at 110°C were modified by the addition of 5–20 mol % silica using incipient wetness impregnation with a solution of tetraethyl orthosilicate in ethanol. Thereafter, the samples were dried in a drying box at 110°C for 12 h and calcined in a muffle furnace at 500–1200°C for 4 h.

The silicon content of the samples was determined by inductively coupled plasma atomic emission spectrometry on an OPTIMA 4300 DV instrument (Perkin Elmer, United States). The concentration of sulfate ions was determined on an ARL-Advant'x X-ray fluorescence analyzer with a Rh anode (Thermo Fisher Scientific, Switzerland). The concentration of ammonium ions was determined by the Kjeldahl method [19].

The X-ray diffraction analysis of the samples was carried out on a URD-63 diffractometer (Freiberg, Germany) with monochromatic CuK_α radiation, by point scanning (a step of 0.05 deg; accumulation time, 10 s at a point) in the range of $2\theta = 10°–70°$. The lattice parameters of γ- and δ-Al_2O_3 were measured with the use of the (440) reflection (for δ-Al_2O_3 in the approximation of a pseudocubic cell) according to the POLIKRISTALL program [20]. Error in the determination of unit cell parameters was ±0.003 Å.

The thermal analysis (TA) of the samples was performed using a NETZSCH STA 449C Jupiter instrument (NETZSCH, Germany) in the temperature range of 20–1500°C with a heating rate of 10 K/min. The sample weight was 100 mg.

The TEM images of the samples were obtained on a JEM 2010 microscope (Jeol, Japan) with a resolution of 1.4 Å and an accelerating voltage of 200 kV. The elemental analysis of the samples was carried out with the use of a microanalytical attachment with an EDAX DX-4 energy-dispersive X-ray detector (Ametek, United States). The analyzed surface area was 150–200 nm^2, and the sensitivity of silicon detection was 0.1 at %.

The IR spectra of the initial sample of γ-Al_2O_3 calcined at 550 and 800°C and the sample of γ-Al_2O_3 modified with 10 mol % silica and calcined at the same temperatures were measured on a Shimadzu FTIR-8300 spectrometer (Shimadzu, Japan) in the region of 2500–3800 cm^{-1} (the region of the stretching vibrations of the hydroxyl groups); the resolution was 4 cm^{-1}, and the number of accumulated spectra was 50. The spectra were normalized to the density of a pellet. Before the measurement, the samples were pressed as pellets with a density of 0.01–0.03 g/cm^2, placed in an IR cell, and kept in a vacuum at 450°C and a residual pressure of $\leq 10^{-3}$ Torr for 2 h.

The specific surface area S (m^2/g) was measured using the thermal desorption of argon at four sorption equilibrium points on SORBI-M instrument (META, Russia).

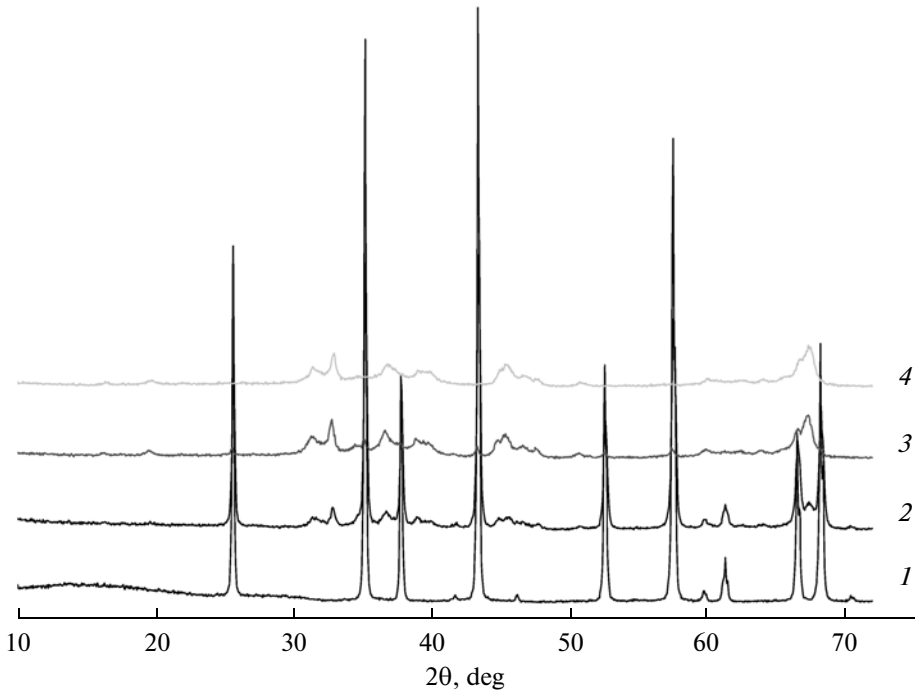

Fig. 2. X-ray diffraction patterns of (*1*) the initial aluminum oxide sample and the samples of aluminum oxide modified with the following amounts of silica (mol %) and calcined at 1200°C: (*2*) 5, (*3*) 15, and (*4*) 20.

The pore structure of the samples was studied by the low-temperature (77 K) sorption of nitrogen on a DigiSorb-2600 instrument (Micromeritics, United States). Before the sorption experiments, the samples were kept in a vacuum of 10^{-4} Torr at 200°C for 5 h.

The mesopore size distribution was calculated from the desorption branch of the isotherm of nitrogen sorption using the classical Barrett–Joyner–Hallenda (BJH) method [21].

RESULTS AND DISCUSSION

According to chemical analysis data, the initial sample of alumina xerogel had the chemical composition $Al_2O_3 \cdot 1.21\ H_2O \cdot 0.022\ SO_4^{2-} \cdot 0.005\ NH_4^+$. According to X-ray diffraction data, it was pseudoboehmite. electron microscopic data showed that the initial sample consisted of coalesced fine-particle lamellar particles with a size of about 1.5–3.0 nm united into aggregates of sufficiently large sizes. The packing of particles in these aggregates was loose; because of this, a considerable pore volume of ~1.6 cm^3/g was formed in the sample (Fig. 1).

Table 1 summarizes X-ray analysis data for aluminum oxide containing no additives and alumina samples modified with silica. It is evident that the modification leads to an increase in the thermal stability of the γ- and δ-Al_2O_3 phases; the higher the concentration of the modifying additive, the greater this increase. Thus, the structural rearrangement of γ-Al_2O_3 into δ-Al_2O_3 in aluminum oxide containing no additives was observed already at a temperature of 950°C and the formation of α-Al_2O_3 was detected at 1100°C, whereas the temperature at which the δ-Al_2O_3 phase in the samples with the addition of 15–20 mol % SiO_2 increased by 150°C and this phase remained stable up to 1200°C (Fig. 2).

These results are confirmed by thermal analysis data, which are given in Fig. 3. From these data, it follows that the weight of the initial aluminum oxide gradually decreased as the temperature was increased up to 1300°C; this can be indicative of the lability of chemical composition in this temperature interval. For aluminum oxide containing no additives, the DTA curve exhibited two endo effects at temperatures of 135 and 448°C (Fig. 3a) accompanied by a significant sample weight loss in the TG and DTG curves. From a comparison between thermal and X-ray diffraction analysis data, we can assume that the observed endo effects are caused by dehydration and the formation of the γ-Al_2O_3 phase. This result is also consistent with published data for aluminum oxide obtained by other methods, for example, from aluminum nitrate [12]. The weight loss in the TG curve and the minimum in the DTG curve in the region of 683 and 1002°C can be caused by the release of residual sulfate of ions and further dehydration, which leads to the formation of the δ-Al_2O_3 phase, as follows from X-ray diffraction analysis data. The formation of the δ-Al_2O_3 phase occurs in this temperature range (Table 1). The high-temper-

Table 1. Effect of silica on the phase composition and structure characteristics of aluminum oxide samples upon thermal treatment in air

Chemical composition of the samples, mol % SiO_2/Al_2O_3	Calcination temperature, °C	Phase composition of Al_2O_3	Unit cell parameters, Å	Unit cell volume V, Å^3
Al_2O_3	500	γ	$a = 7.929$	498.40
	800	γ	$a = 7.924$	497.50
	950	δ	$a = 7.915$	495.80
	1000	δ	$a = 7.880$	489.90
	1100	α	$a = 4.758$	293.60
			$c = 12.972$	
		δ	$a = 7.870$	487.40
	1200	α	$a = 4.756$	293.53
			$c = 12.977$	
5% SiO_2/Al_2O_3	500	γ	$a = 7.936$	499.80
	800	γ	$a = 7.917$	496.20
	1000	δ	$a = 7.890$	491.20
	1100	α	$a = 4.756$	293.30
			$c = 12.965$	
		δ	$a = 7.878$	488.90
	1200	α	$a = 4.756$	293.30
			$c = 12.965$	
		δ	$a = 7.870$	487.40
10% SiO_2/Al_2O_3	500	γ	$a = 7.939$	500.40
	800	γ	$a = 7.913$	495.80
	1000	γ	$a = 7.900$	493.00
	1100	δ	$a = 7.886$	490.42
		α, traces		
	1200	δ	$a = 7.886$	490.42
		α	$a = 4.755$	293.13
			$c = 12.965$	
15% SiO_2/Al_2O_3	500	γ	$a = 7.949$	502.30
	800	γ	$a = 7.924$	497.50
	1000	γ	$a = 7.910$	494.90
	1100	δ	$a = 7.889$	491.00
	1200	δ	$a = 7.866$	486.70
		α, traces	$a = 4.758$	294.80
			$c = 13.022$	
20% SiO_2/Al_2O_3	500	γ	$a = 7.954$	503.20
	800	γ	$a = 7.935$	499.60
	1000	γ	$a = 7.915$	495.90
	1100	δ	$a = 7.898$	492.80
	1200	δ	$a = 7.865$	486.50

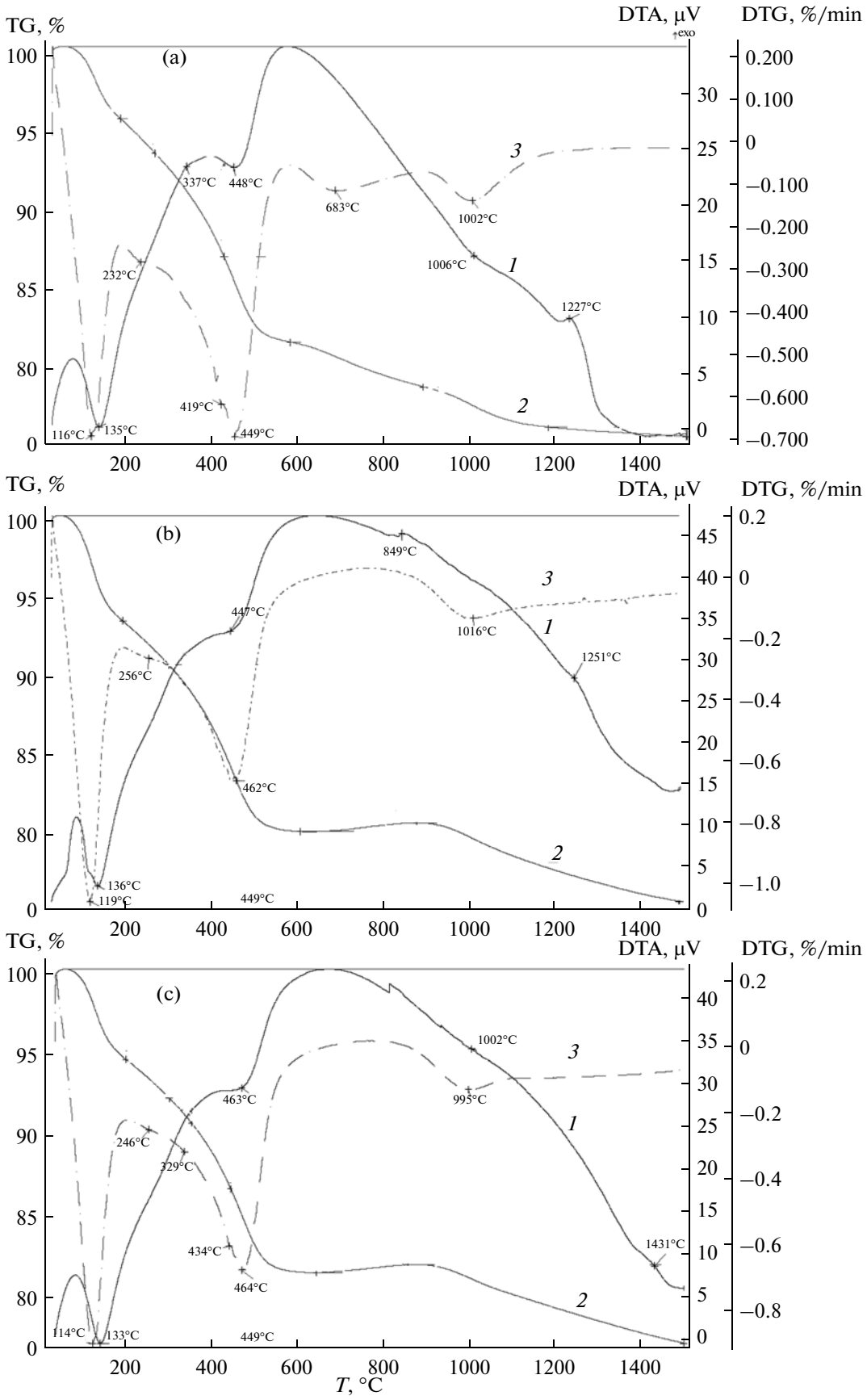

Fig. 3. Thermal analysis data for (a) the initial aluminum oxide sample and the samples of aluminum oxide modified with the following amounts of silica, mol %: (b) 10 and (c) 20. (*1*) DTA; (*2*) TG; and (*3*) DTG.

ature exo effect in the region of 1270°C is due to the formation of the α-Al_2O_3 phase in accordance with X-ray diffraction analysis data and published data [12]. Note that the temperature of the formation of the α-Al_2O_3 phase derived from the thermoanalytical data is higher than the temperature of the phase transition δ-$Al_2O_3 \rightarrow \alpha$-$Al_2O_3$, determined from the X-ray diffraction analysis data. This was likely due to different kinetics of the phase transition process under various conditions of heat treatment.

For the aluminum oxide sample containing 10 mol % SiO_2, the temperature of endo effects in the DTA curve in the region of 135 and 447°C, which are accompanied by a weight loss in the TG curve, does not change in comparison with the initial sample, whereas for the sample containing 20 mol % SiO_2 the temperature of the second endo effect, which is caused by the loss of structural water and the formation of the γ-Al_2O phase, increased by 15°C (Figs. 3b, 3c). In this case, as can be seen in the DTG and TG curves, no changes in the weights of these samples were observed in a fairly wide temperature range of 550–850°C, and then the weight gradually decreased as the temperature was further increased. Furthermore, modification with silica shifts the high-temperature exo effect due to the formation of the α-Al_2O_3 phase to higher temperatures. This shift increases with an increasing concentration of silicon oxide in the sample. Thus, for the sample containing 20 mol % SiO_2, the temperature of the formation of the α-Al_2O_3 phase increased by 160°C, as compared with the initial aluminum oxide, and was 1431°C. Thus, from X-ray diffraction and thermal analysis data, it follows that the modification of aluminum oxide leads to a shift of phase transition temperatures in the series γ-$Al_2O_3 \rightarrow \delta$-$Al_2O_3 \rightarrow \alpha$-$Al_2O_3$ to the high-temperature region increasing the thermal stability of the fine-particle of γ- and δ-Al_2O_3 phases. For explaining the reasons for this stabilization, special attention was given to a study of the real structure of the samples.

A comparison between the cubic lattice parameters a in the initial γ-Al_2O_3 sample and the samples modified with silica, which also had the structure of γ-Al_2O_3, calcined at 500°C demonstrated that the lattice parameter a increased with an increasing concentration of the additive (Table 1). Thus, the parameter a in the sample of γ-Al_2O_3 with no additives was 7.929 Å, and it was 7.954 Å in the sample of γ-Al_2O_3 containing 20 mol % SiO_2. A further increase in the temperature of calcination of aluminum oxide, either containing no additives or modifoed with silica, resulted in a gradual decrease in the parameter a of the γ- and δ-Al_2O_3 phases. Note that a less sharp decrease in the lattice parameter a with calcination temperature was observed as the additive content was increased. In any event, the greater the silica content, the greater the parameter a for samples with the structures of γ- and δ-Al_2O_3 calcined at the same temperature. Moreover, the replacement of aluminum ions by silicon ions in the lattice of γ- or δ-Al_2O_3 should not lead to an increase in the crystal lattice parameter because the ionic radius of Si^{4+} is smaller than the ionic radius of Al^{3+} [22].

Based on the simulation of X-ray spectra and electron microscopic data, it was demonstrated [15–17] that aluminum oxide obtained at a calcination temperature of about 500–600°C is really the oxo–hydroxo compound Al_3O_4OH, which is characterized by a high concentration of planar defects stabilized by hydroxyl groups. An increase in the calcination temperature leads to the gradual loss of the hydroxyl groups and a decrease in the concentration of related planar defects and further to the ordering of defects and the formation of δ-Al_2O_3 and then α-Al_2O_3. Taking into account these data and the results of TA, which show a decrease in the weight of the test sample of γ-Al_2O_3 in the range of 500–1200°C, we hypothesize that a decrease in the lattice parameter a of γ- and δ-Al_2O_3 phases, which was observed as the calcination temperature was increased, can be due to the gradual loss of hydroxyl groups and the formation of a more ordered structure. The less sharp decrease in the parameter a of modified aluminum oxide, as compared with that of the initial sample, can be attributed to the higher thermal stability of hydroxyl groups, which stabilize defects in the structure of γ-Al_2O_3. Probably, this can be due to the partial replacement of aluminum ions by silicon ions in the structure of γ-Al_2O_3 in the region of defects where the structure is more disordered. To test this hypothesis, we studied the microstructure and the state of hydroxyl groups in the samples of aluminum oxide containing no additives and also modified with silicon.

Figure 4 shows the micrographs of an aluminum oxide sample calcined at 550°C. It is evident that this sample consisted of coalesced lamellar particles of size from 10 to 80 nm with a thickness of 2–5 nm (Fig. 4a). In the most developed plane (110), the structure consisted of joined extensive blocks with a transverse size of 1–3 nm, oriented in the [111] direction. The structure of the extensive blocks is sufficiently strongly disordered, and it consists of domains of size 1–3 nm joined to each other in incoherent and coherent manners (Fig. 4b). In the plane perpendicular to the plane (110), the coalescence of plates occurs with the formation of planar defects (Fig. 4c). After calcination at 1100°C, the micrograph mainly exhibited large oxide particles of α-Al_2O_3 with a regular structure with sizes of 100–300 nm (Figs. 5a, 5b) and an impurity of the more dispersed particles of δ-Al_2O_3 with the size to 40 nm (Fig. 5c), which is consistent with X-ray diffraction analysis data. The structure of the sample of δ-Al_2O_3 calcined at 1100°C is sufficiently regular.

Figure 6 shows the micrographs of an aluminum oxide sample containing 15 mol % SiO_2 calcined at 550°C. It is evident that the morphology of this sample is similar to that of the aluminum oxide sample without additives, and, according to microanalysis data, silicon is uniformly distributed in the sample. The study of the microstructure of this sample (Fig. 6b) showed that, in the most developed plane (110), the structure consists of joined extensive blocks oriented in the [111] direction with the formation of extensive defects between them. However, the blocks are much smaller than the blocks of the initial aluminum oxide, and they are not greater than 1.5 nm. The structure of the blocks is almost completely disordered. The thickness of the joined lamellar particles in the plane perpendicular to the plane (110) was mainly no greater than 2 nm.

In the micrograph of the modified aluminum oxide (Fig. 7), it can be seen that thermal treatment at a temperature of 1100°C leads to the larger coalescences of lamellar particles and an increase in their thickness to ~9–10 nm. Simultaneously, the coalescence of particles occurred in the most developed plane (110) due to the formation of interblock boundaries between them; the structure ordered with the retention of the block structure with a block width of 1.5–2 nm. According to electron microscopic and X-ray diffraction analysis data, the sample corresponds to δ-Al_2O_3.

Figures 8 and 9 show the IR spectra of pure γ-Al_2O_3 samples the same samples containing 10 mol % silica, both calcined at 550 and 800°C, in the region of the stretching vibrations of OH groups. The same set of hydroxyl groups was present in the spectra of the γ-Al_2O_3 sample: four types of bridging groups characterized by the absorption bands ν(OH) at 3670, 3685, 3700, and 3730 cm^{-1} and three types of terminal groups characterized by absorption bands at 3750, 3775, and 3792 cm^{-1} [23, 24]. An increase in the temperature leads to a decrease in the intensity of all types of absorption bands due to OH groups. Three types of bridging hydroxyl groups with absorption bands at 3750, 3775, and 3792 cm^{-1} and two types of terminal hydroxyl groups with absorption bands at 3775 and 3792 cm^{-1} are observed in the IR spectra of the γ-Al_2O_3 sample modified with silica. Furthermore, an absorption band at 3745 cm^{-1} additionally appears in the spectra; this absorption band can be due to the terminal Si–OH group [23, 25]. As the calcination temperature of this sample was increased, the intensity of all types of absorption bands decreased to indicate its partial dehydration. Consequently, the modification of aluminum oxide leads to the appearance of the Si–OH group, which is characterized by a higher bond atrength than the Al–OH groups [23, 26]. Thus, it is well known that Si–OH groups possess high heat resistance; they are observed on the surface of silica gel upon heat treatment up to 1400°C. It is likely that this factor plays an important role in an increase in the thermal stability of the structure of the fine-particle forms of γ- and δ-Al_2O_3.

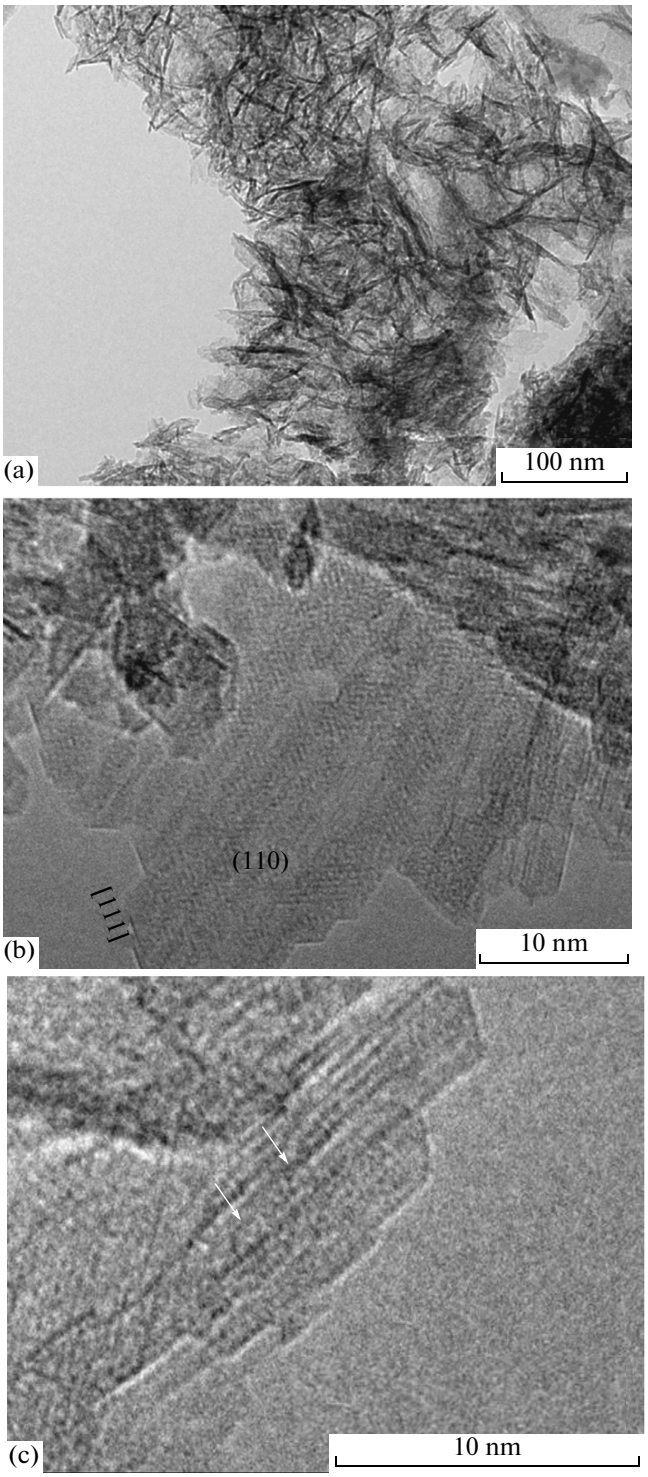

Fig. 4. Micrographs of aluminum oxide calcined at 550°C: (a) general view and (b, c) microstructure.

Figure 10 plots the dependence of the specific surface area of the samples on calcination temperature.

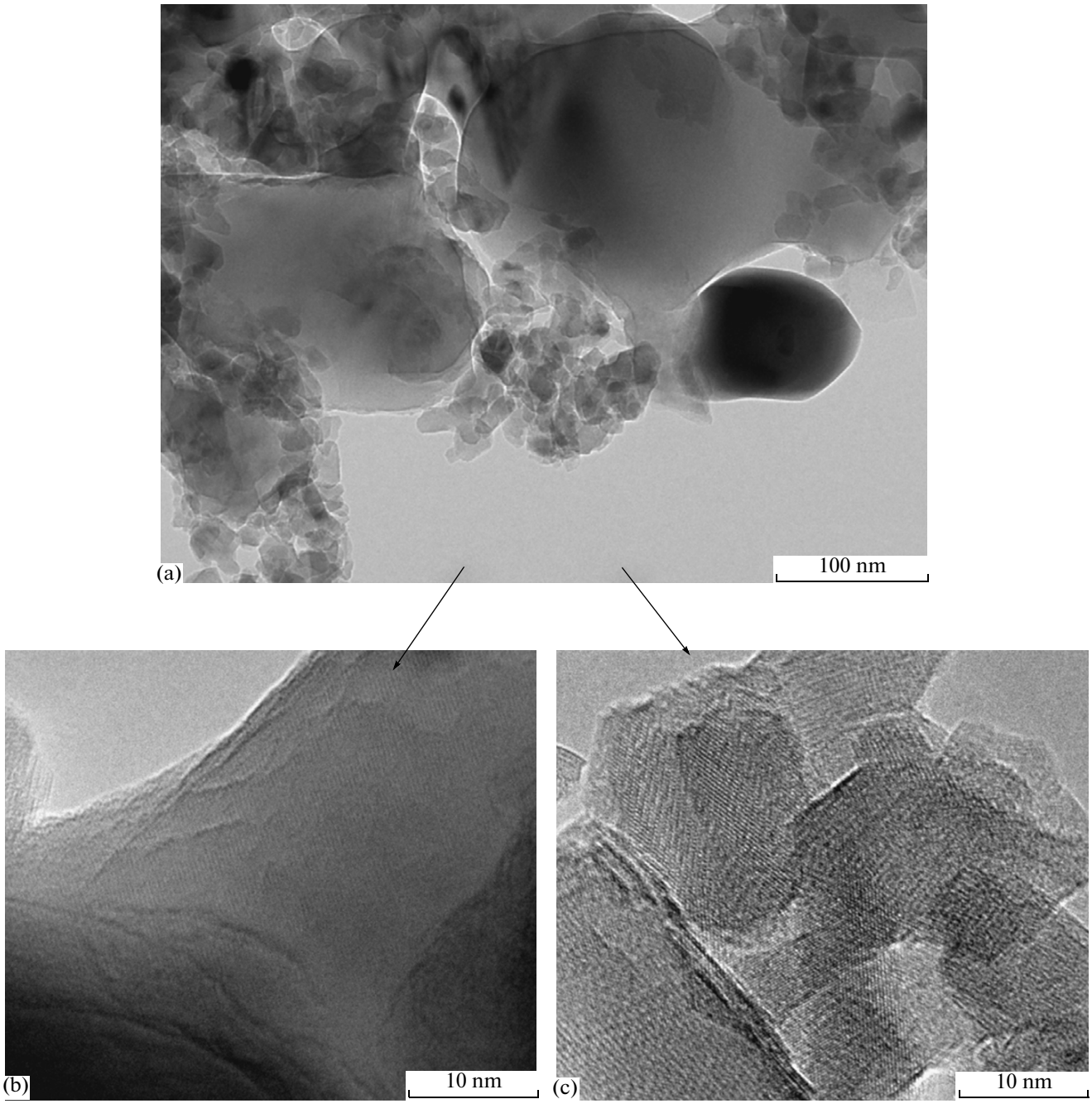

Fig. 5. Micrographs of aluminum oxide calcined at 1100°C: (a) general view and the structures of (b) α-Al_2O_3 and (c) δ-Al_2O_3 particles.

The specific surface area of the initial aluminum oxide dried at 110°C was 300 m^2/g, and then it dramatically decreased with temperature and did not exceed 5 m^2/g after calcination at 1200°C. The specific surface areas of the modified aluminum oxide samples calcined below 400°C was lower than that of aluminum oxide without additives; this can be due to the presence of undecomposed tetraethyl orthosilicate in the pores of the modified samples. As the temperature was increased to 500–600°C, the surface areas of all samples increased to reach a maximum value, whereas a decrease in the surface area was observed at a temperature higher than 600°C. At the same time, the specific surface areas of the samples containing silica were higher than that of the initial aluminum oxide at the same calcination temperatures. In this case, an increase in the concen-

tration of the modifying additive caused the retention of the higher value of the specific surface area in a wide range of calcination temperatures. Note that a fairly high specific surface area (about 50 m^2/g) can be conserved by modification of aluminum oxide with silica even after the calcination of the samples at 1200°C, whereas the specific surface area of aluminum oxide without the additives is lower by an order of magnitude.

The data presented in Table 2 indicate that the modification of aluminum oxide also leads to the retention of a higher mesopore volume at temperatures of 800–1100°C. Figure 11 shows the differential curves of mesopore volume distribution according to pore sizes. It can be seen that, at calcination temperatures of 800, 1000, and 1100°C, an increase in the concentration of silica in aluminum oxide leads to the retention of mesopores with a smaller diameter (D) and the formation of a more developed pore structure. A comparison of the above results with X-ray diffraction analysis data indicates that these texture changes at high calcination temperatures can be due to the increase in the thermal stability of the γ- and δ-Al_2O_3 phases.

Thus, the results of this study demonstrate that the modification of aluminum oxide with silica leads to an increase in the thermal stability of the γ- and δ-Al_2O_3 phases; because of this, they retain high specific surface areas and developed pore structure at high calcination temperatures. The experimental results and published data [15–17] make it possible to assume that the increase in the thermal stability of the metastable γ- and δ-Al_2O_3 phases in the presence of silica can be due to a change in their real structure, namely, an increase in the concentration of extensive defects stabilized by hydroxyl groups, which leads to a significant structure disordering. As follows from data on the study of a hydroxyl cover, the appearance of the hydroxyl groups bound to silicon atoms Si–OH, which are characterized by higher bond strength in comparison with the hydroxyl groups bound to aluminum atoms Al–OH, was detected in the alumina sample containing silica. It is likely that the Si–OH hydroxyl groups, which are more thermally stable that the Al–OH hydroxyl groups, stabilize the microstructure of γ- and δ-Al_2O_3 to higher temperatures. These conclusions are consistent with published data [15–17], which indicate that packets with the structure of spinel $[Al_3O_4]^+$ are the building blocks of all of the low-temperature forms of aluminum oxide. These packets form electrically neutral lamellar domains with the developed plane (110) or (111) to 1 nm in thickness with a size to 5 nm in the developed plane. An electrically neutral particle with the ratio Al : O = 2 : 3 in the bulk is considered the primary particle. If the number of cations is smaller than 2, then electroneutrality is ensured by additional OH groups. The 2 : 3 sto-

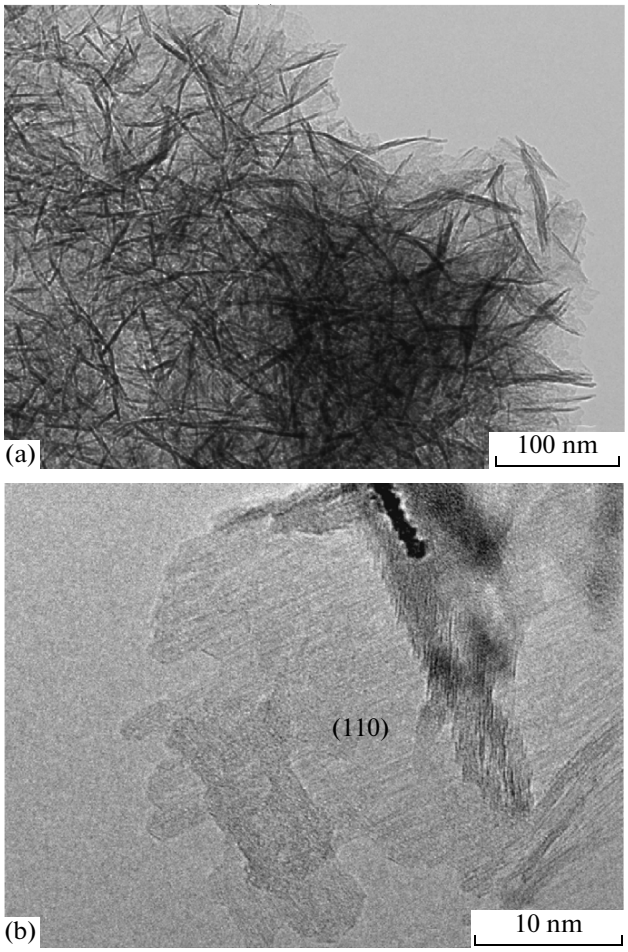

Fig. 6. Micrographs of aluminum oxide modified with 15 mol % silica calcined at 550°C: (a) general view and (b) microstructure.

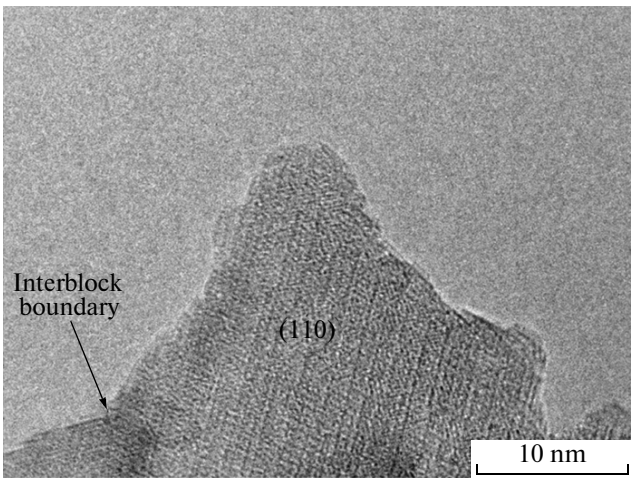

Fig. 7. Micrograph of the aluminum oxide sample modified with 15 mol % silica calcined at 1100°C.

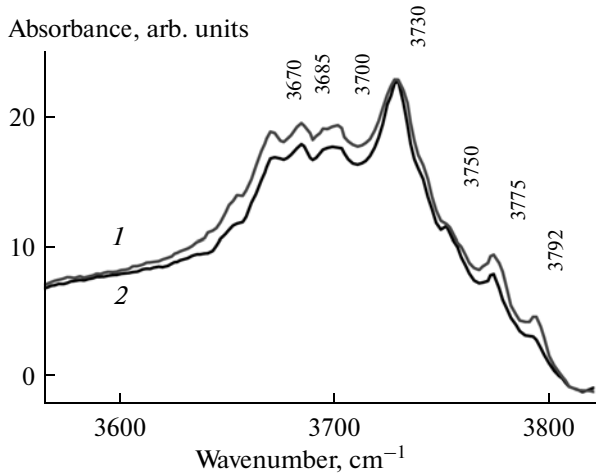

Fig. 8. IR spectra of γ-Al_2O_3 samples calcined at (*1*) 550 and (*2*) 800°C in the region of the stretching vibrations of OH groups.

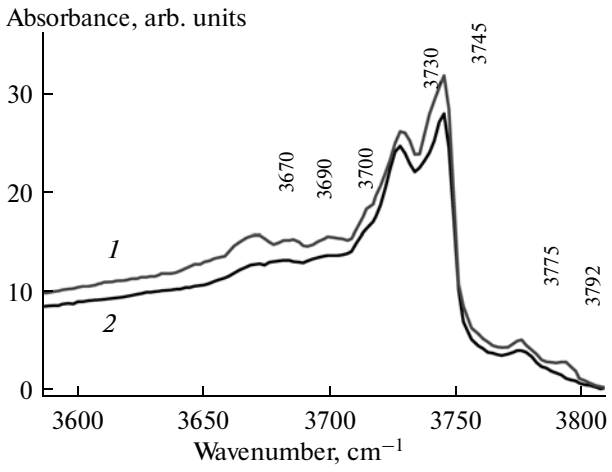

Fig. 9. IR spectra of γ-Al_2O_3 samples modified with 10 mol % silica and calcined at (*1*) 550 and (*2*) 800°C in the region of the stretching vibrations of OH groups.

ichiometry appear because of the presence of planar defects, primarily, the systems of planes (110) formed due to a shift of layers by a half-dislocation vector. The jointing of two domains with the structure of $[Al_3O_4]^+$ shifted relative to each other occurs with the loss of a cation layer, which can be represented as the jointing of two domains at planes of the (110) type through an excess layer of oxygen: $2[Al_3O_4]^+[2O^{2-}]2[Al_3O_4]^+$ (the Al_2O_3 composition). The simulation of the structure of γ-Al_2O_3 shows that the ratio of cations and anions in it composes $Al_{2.4}O_4$ or $Al_{1.8}O_3$, as a result of which the O^{2-} ions in the excess layer are replaced by OH^- ions. The O^{2-} composition results from the complete replacement of OH^- by $[Al_3O_4]^+[2OH)^-][Al_3O_4]^+$. Consequently, the samples calcined at 500–600°C are in reality the oxo–hydroxo compounds Al_3O_4OH. Calcination at higher temperatures leads to a gradual loss of residual hydroxyl groups, a decrease in the concentration of related planar defects, and then an ordering of defects with the formation of the δ-Al_2O_3phase and then α-Al_2O_3. It is, therefore, likely that the increase in the thermal stability of hydroxyl groups in γ-Al_3O_4 modified with silicon oxide leads to the stabilization of defects in its structure and the retention of its microstructure to higher temperatures in comparison with the initial aluminum oxide.

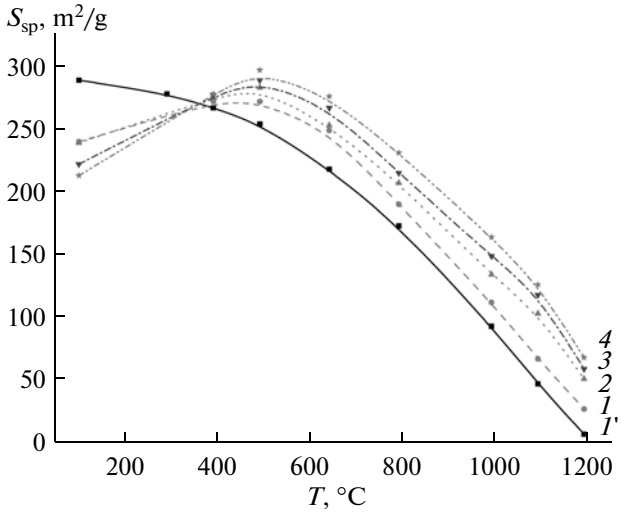

Fig. 10. Effect of calcination temperature on the specific surface areas of (*1'*) aluminum oxide containing no additives and aluminum oxide modified with the following amounts of silica, mol %: (*1*) 5, (*2*) 10, (*3*) 15, and (*4*) 20.

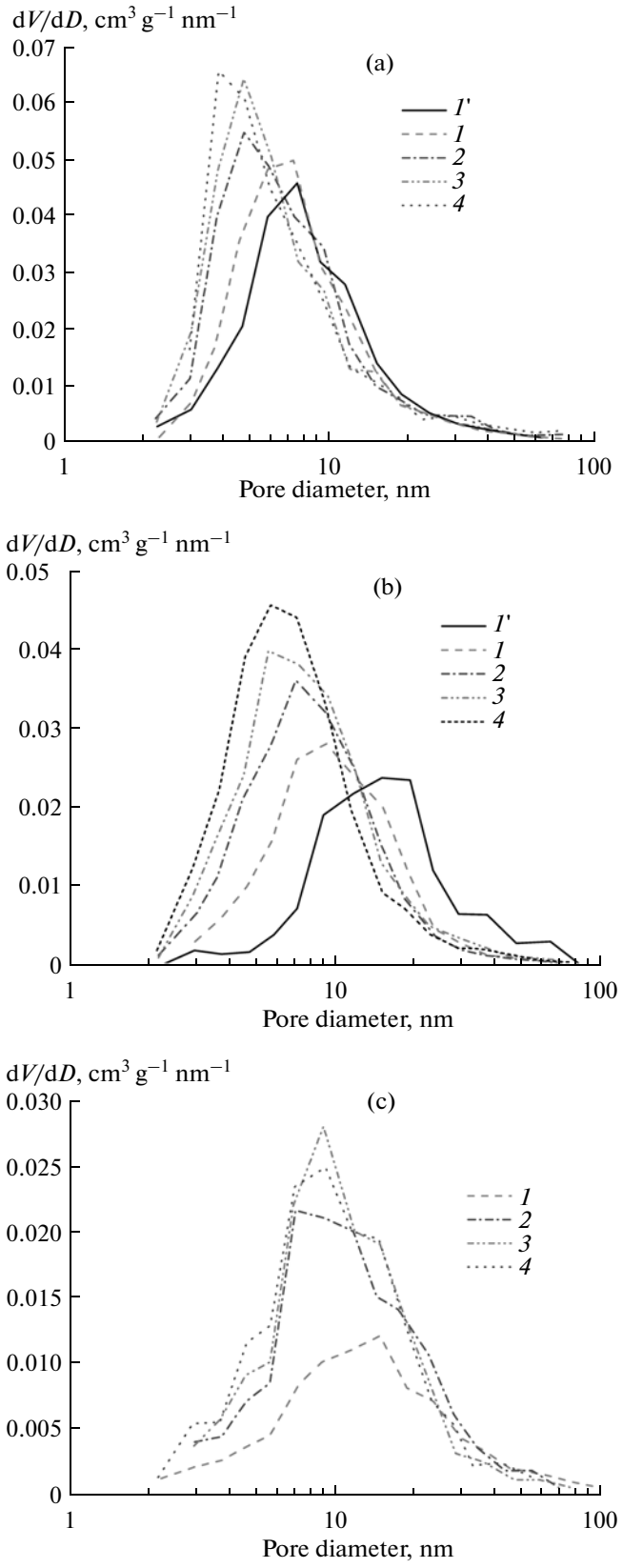

Fig. 11. Pore size distribution for aluminum oxide samples (*1'*) containing no additives and modified with the following amounts of silica, mol %: (*1*) 5, (*2*) 10, (*3*) 15, and (*4*) 20. The samples were calcined at temperatures of (a) 800, (b) 1000, and (c) 1100°C.

Table 2. Texture of silica-modofoed aluminum oxide samples calcined at 800–1100°C (S is the specific surface area; V_s is the mesopore volume; and D is the predominant mesopore diameter calculated by the BJH method)

Chemical composition of the samples, mol % SiO_2/Al_2O_3	S, m^2/g			V_s, cm^3/g			D, nm		
	Temperature, °C								
	800	1000	1100	800	1000	1100	800	1000	1100
Al_2O_3	167	81	15	0.583	0.369	–	7.7	9.7	–
5% SiO_2/Al_2O_3	187	109	68	0.574	0.430	0.345	7.4	9.3	15
10% SiO_2/Al_2O_3	213	132	108	0.633	0.447	0.442	4.8	7.2	7.2
15% SiO_2/Al_2O_3	206	150	119	0.600	0.520	0.457	4.8	5.7	9.2
20% SiO_2/Al_2O_3	223	178	127	0.623	0.550	0.462	3.9	5.8	9.4

ACKNOWLEDGMENTS

We are grateful to A.V. Ishchenko and I.G. Danilova for performing the electron microscopic and IR spectroscopic measurements.

This work was supported by the Siberian Branch of the Russian Academy of Sciences (interdisciplinary project no. 36) and by the program "Development of the Scientific Potential of Higher School" of the Ministry of Education and Science of the Russian Federation (project no. 2.1.1./10165).

REFERENCES

1. Pines, H. and Haag, W.J., *J. Am. Chem. Soc.*, 1961, vol. 83, p. 2847.
2. Taylor, K.C., *Catal. Rev.*, 1993, vol. 35, no. 4, p. 457.
3. Belton, D.N. and Taylor, K.C., *Curr. Opin. Solid State Mater. Sci.*, 1999, vol. 4, p. 97.
4. Martinez-Arias, A., Fernandez-Garcia, M., Iglesias-Juez, A., Hungrá, A.B., Anderson, J.A., Conesa, J.C., and Soria, J., *Appl. Catal., B*, 2001, vol. 31, p. 51.
5. Klimov, O.V., Fedotov, M.A., Pashigreva, A.V., Budukva, S.V., Kirichenko, E.N., Bukhtiyarova, G.A., and Noskov, A.S., *Kinet. Catal.*, 2009, vol. 50, no. 6, p. 867.
6. Ballod, L.A. and Topchieva, K.V., *Usp. Khim.*, 1951, vol. 20, no. 2, p. 161.
7. Espie, A.W. and Vickerman, J.C., *J. Chem. Soc., Faraday Trans. 1*, 1984, vol. 80, no. 7, p. 1903.
8. Dai, W.L., Gao, Y., Ren, L.P., Yang, X.L., Xu, J.H., Li, H.X., He, H.Y., and Fan, K.N., *J. Catal.*, 2004, vol. 228, p. 80.
9. Gervasini, A., Manzoli, M., Martra, G., Pointi, A., Ravasio, N., Sordelli, L., and Zaccheria, F., *J. Phys. Chem. B*, 2006, vol. 110, p. 7851.
10. Bennici, S., Gervasini, A., Ravasio, N., and Zaccheria, F., *J. Phys. Chem. B*, 2003, vol. 107, p. 5168.
11. Pang, W.W., Zhang, Y.Z., Choi, K.-H., Lee, J.K., Yoon, S.H., Mochida, I., and Nakano, K., *Pet. Sci. Technol.*, 2009, vol. 27, no. 12, p. 1349.
12. Kul'ko, E.V., Ivanova, A.S., Litvak, G.S., Kryukova, G.N., and Tsybulya, S.V., *Kinet. Catal.*, 2004, vol. 45, no. 5, p. 714.
13. Ivanova, A.S., Litvak, G.S., Kryukova, G.N., Tsybulya, S.V., and Paukshtis, E.A., *Kinet. Catal.*, 2000, vol. 41, no. 1, p. 122.
14. Kryukova, G.N., Klenov, D.O., Ivanova, A.S., and Tsybulya, S.V., *J. Eur. Ceram. Soc.*, 2000, vol. 20, p. 1187.
15. Tsybulya, S.V. and Kryukova, G.N., *Phys. Rev. B: Condens. Matter*, 2008, vol. 77, no. 2, p. 1098.
16. Tsybulya, S.V., *Doctoral (Phys.–Math.) Dissertation*, Novosibirsk: Inst. of Inorganic Chemistry, 2004.
17. Sheffer, K.I., *Cand. Sci. (Chem.) Dissertation*, Novosibirsk: Novosibirsk: Inst. of Inorganic Chemistry, 2008.
18. Digne, M., Revel, R., Boualleg, M., Chiche, D., Rebours, B., Moreaud, M., Celse, B., Chaneac, C., and Jolivet, J.-P., *Stud. Surf. Sci. Catal.*, 2010, vol. 175, p. 127.
19. Kolthoff, M. and Sandell, E.B., *Textbook of Quantitative Inorganic Analysis*, New York: Macmillan, 1936.
20. Tsybulya, S.V., Cherepanova, S.V., and Solov'eva, L.P., *Zh. Strukt. Khim.*, 1996, vol. 37, no. 2, p. 379.
21. Barret, E.P., Joyner, L.G., and Hallenda, P.H., *J. Am. Chem. Soc.*, 1951, vol. 73, no. 1, p. 373.
22. *Kataliticheskie svoistva veshchestv: Spravochnik* (Catalytic Properties of Substances: A Handbook), Roiter, V.A., Ed., Kiev: Naukova Dumka, 1968.
23. Paukshtis, E.A., *Infrakrasnaya spektroskopiya v geterogennom kislotno-osnovnom katalize* (Infrared Spectroscopy Applied to Heterogeneous Acid–Base Catalysis), Novosibirsk: Nauka, 1992.
24. Glazneva, T.S., Kotsarenko, N.S., and Paukshtis, E.A., *Kinet. Catal.*, 2008, vol. 49, no. 6, p. 859.
25. Kazanskii, V.B., *Kinet. Katal.*, 1980, vol. 21, no. 1, p. 159.
26. Mikheikin, N.D., Abronin, M.A., and Zhidomirov, G.M., *Kinet. Katal.*, 1978, vol. 19, no. 4, p. 1050.